*Clays and Clay Minerals*, Vol. 63, No. 1, 15–29, 2015.

# REVISITING THE INFRARED SPECTRUM OF THE WATER–SMECTITE INTERFACE

ARTUR KULIGIEWICZ[1], ARKADIUSZ DERKOWSKI[1,*], MAREK SZCZERBA[1], VASSILIS GIONIS[2], AND GEORGIOS D. CHRYSSIKOS[2]

[1] Institute of Geological Sciences, Polish Academy of Sciences, ul. Senacka 1, 31-002 Krakow, Poland
[2] Theoretical and Physical Chemistry Institute, National Hellenic Research Foundation, 48 Vassileos Constantinou Av., Athens 11635, Greece

**Abstract**—An overlap of bands produced by the O–H stretching vibrations of $H_2O$ (O–$H_w$) and structural OH (O–$H_s$) in smectite hampers the study by infrared spectroscopy (IR) of both their layer and interlayer structure. The present study re-evaluated the $D_2O$ saturation of smectite as a tool to enable separation of the overlapping bands at ambient conditions. Real-time monitoring by Attenuated Total Reflectance infrared spectroscopy (ATR-IR) was employed during *in situ* sample drying and $H_2O$ or $D_2O$ saturation at ambient temperature. Six dioctahedral and one trioctahedral pure smectites in $Ca^{2+}$-, $Na^{+}$-, and $Cs^{+}$-cationic forms were studied to explore variability in total layer charge, charge location, and interlayer cation. The IR data showed the interlayer O–$D_w$ signature at 2700–2200 $cm^{-1}$ as a proxy for the O–$H_w$ signature in the 3700–3000 $cm^{-1}$ region. In addition to the expected liquid-like bands of $D_2O$ in the interlayer, these O–$D_w$ spectra exhibited an additional sharp stretching feature in the 2695–2680 $cm^{-1}$ range. No significant cation dependence of the sharp band position was observed between pairs of Ca- and Na-smectites for relative humidity (RH) between 60 and 80%, despite the large difference in the ionic potential between these interlayer cations. The intensity of the sharp band was found to be almost insensitive to changes in water content within the range 60–80% RH. The sharp band frequency decreased linearly with increasing total charge of the 2:1 layer (and can be used as a proxy for it), but no effect of charge location could be discerned. In agreement with early studies, this band was attributed to $D_2O$ located on the surface of the interlayer, pointing one O–D group toward the siloxane surface. Based on its high frequency, this band was indicative of free O–D oscillators, with very little or no involvement in hydrogen bonding ("dangling OD"). By analogy to the spectra of $D_2O$-smectites, the spectrum of $H_2O$-smectites also involves a sharp O–$H_w$ analog at ~3630 $cm^{-1}$ overlapping with typical $OH_s$ bands (*e.g.* $Al_2OH$). As a result of this overlap, the sharp 3630 $cm^{-1}$ O–$H_w$ contribution was often missed or attributed solely to O–$H_s$.

**Key Words**—Adsorbed Water, ATR, Deuteration, Infrared Spectroscopy, Layer Charge, Smectite.

## INTRODUCTION

Analysis of the mid-IR spectra of clay minerals is often hampered by the overlap of bands originating from structural OH groups ($OH_s$) and OH groups of adsorbed water ($OH_w$) in the O–H stretching region (3700–3000 $cm^{-1}$). Unambiguous distinction between the different types of O–$H_s$ and O–$H_w$ stretching modes of clay mineral samples is a crucial prerequisite for their further systematic investigation by IR. This is especially true in the case of dioctahedral smectites. The lack of distinction between O–$H_s$ and O–$H_w$ in the 3640–3610 $cm^{-1}$ range impedes both the study of interlayer $H_2O$ and the identification of individual O–$H_s$ stretching components, and hence, also, the establishment of correlations between O–$H_s$ stretching and the octahedral-sheet composition (*e.g.* Madejová *et al.*, 1994; Fialips *et al.*, 2002; Petit *et al.*, 2002; Zviagina *et al.*, 2004).

Following the seminal work of V.C. Farmer and his group at the Macaulay Institute, Aberdeen, UK, a number of monographs and review papers have dealt in depth with the application of IR to the identification and structural characterization of clay minerals, raising the issue mentioned above (Farmer, 1974; Russell and Fraser, 1994; Petit *et al.*, 1995; Besson and Drits, 1997; Madejová and Komadel, 2001; Madejová, 2003; Gates, 2005). Early IR research was based mostly on thin self-supported clay films measured in transmission using dispersive instruments fitted with suitable environmental cells. More recent studies have benefited from the advent of Fourier transform spectrometers and Attenuated Total Reflectance (ATR) collection optics offering improved spectral quality, convenient non-invasive spectral acquisition, and new possibilities for real-time monitoring (*e.g.* Johnston *et al.*, 1992; Yan *et al.*, 1996; Ras *et al.*, 2007).

Despite the widespread application of IR to clays and clay-based materials, it appears that some of the early pioneering work is fading out without being followed or challenged by modern findings. Early IR work based on substituting interlayer $H_2O$ with $D_2O$ provided evidence that the sharp, high-frequency bands observed at

* E-mail address of corresponding author:
ndderkow@cyfronet.pl
DOI: 10.1346/CCMN.2015.0630102

~3640–3610 $cm^{-1}$ involve a significant contribution from weakly hydrogen-bonded (H-bonded) adsorbed $O-H_w$ (Russell and Farmer, 1964; Farmer and Russell, 1971; Suquet *et al.*, 1977; Sposito and Prost, 1982; Cariati *et al.*, 1981, 1983; Sposito *et al.*, 1983). More recent assignments of the same high-frequency feature in dioctahedral smectites vary. Some authors adopt the aforementioned assignment of an $O-H_w$ stretching mode (*e.g.* Bishop *et al.*, 1994; Madejová *et al.* 1994) and others assign it only to $O-H_s$, and not $O-H_w$ (Bukka *et al.*, 1992; Xu *et al.*, 2000; Madejová and Komadel 2001).

Substitution of interlayer $H_2O$ with $D_2O$ seemed to offer an elegant solution to the problems described above, as $D_2O$ band positions are shifted by a factor of ~1.36 toward lower wavenumbers. The effectiveness of this technique seemed to be confirmed (Farmer and Russell 1971); $D_2O$ saturation can be considered as useful provided that no deuteration of $OH_s$ is assured. Russell *et al.* (1970) studied *in situ* deuteration of structural OH in a number of smectites. Relatively high temperatures and long reaction times (300–400ºC, 1–14 h) were needed for the complete H/D exchange of the structural OH. The progress of $OH_s$ deuteration was manifested by the growing intensity of the structural δ OD bending modes: $Al_2OD$ was observed at 700–690 $cm^{-1}$, AlFe(III)OD at ~675 $cm^{-1}$, and AlMgOD at ~650 $cm^{-1}$ (compared to the corresponding δ OH modes at ~915, 880, and 840 $cm^{-1}$, respectively). The appearance of these bands in spectra of smectites after saturation with $D_2O$ can be treated as an indicator of $OH_s$ deuteration. Some effects interpreted as partial deuteration of $OH_s$ were, however, observed at lower temperatures (98ºC, Bukka *et al.*, 1992).

The aim of the present study was to re-evaluate $D_2O$ saturation as a convenient spectrochemical tool for the separation of the $O-H_s$ and $O-H_w$ ($O-D_w$) stretching modes of smectite at ambient hydration conditions. Seven smectite samples in three cation-exchanged forms were selected to represent most of the variability found in nature. The spectrum of water (as $D_2O$) was obtained free from the interference of structural OH groups and analyzed in terms of layer charge, charge location, and exchangeable cation.

## EXPERIMENTAL

### *Materials*

The present study was based on six natural dioctahedral smectites from the collection of the Source Clays Repository of The Clay Minerals Society and one synthetic saponite (Table 1). SCa-3 and SAz-2 are high-charge montmorillonites with almost no tetrahedral charge. SWy-2 (Wyoming) is a low-charge beidellitic montmorillonite. SWa-1 is a low-charge Fe-rich smectite/nontronite with almost equal amounts of tetrahedral and octahedral charge. SbCa-1 and SbId-1 are beidellites with high and low charges, respectively. The synthetic saponite (SAP) is a high-charge member of the trioctahedral series reported by Pelletier *et al.* (2003).

All dioctahedral smectite samples were purified by removing carbonates, organics, and Fe-oxides/hydroxides (except SWa-1) by a sequence of acetic acetate buffer, peroxide, and buffered sodium dithionite treatments (Jackson, 1969). Subsequently, particle-size fractions were separated by centrifugation and dialyzed in deionized water. All fine fractions were found to be mineralogically pure, with the exception of SbId-1 which contained a kaolinite admixture, clearly evident in the IR spectra. Homoionic forms of each smectite were prepared by five washings with appropriate 0.5 M $Ca^{2+}$, $Na^+$, and $Cs^+$ chloride solutions of reagent-grade purity and dialysis in deionized water.

The literature on smectite samples from the Source Clays Repository reports various size fractions with different mineral formulae and layer-charge density (*e.g.* Zviagina *et al.*, 2004; Gates, 2005). Moreover, the determination of the total exchangeable cations as a way to measure layer-charge density is method-dependent (Wolters *et al.*, 2009) and literature values may not be comparable to each other unless determined by the same method. For these reasons, the total layer charge per half unit cell ($Q_{tot}$) of the actual particle fractions used in the study was determined independently (Table 1). This charge determination was based on the measurement of the Na content in the Na-exchanged samples subjected to conventional acid digestion, using a flame photometer (Sherwood 420 by Sherwood Scientific Ltd., Cambridge, UK) calibrated against NIST standards 76a and 70a.

Table 1. Smectites used in the study.

| Sample | Layer type | Charge location | Particle size fraction | Total layer charge $Q_{tot}$ |
|---|---|---|---|---|
| SCa-3 | montmorillonite | octahedral | <1.0 μm | 0.51(1) |
| SAz-2 | montmorillonite | octahedral | <2.0 μm | 0.52(1) |
| SWy-2 | montmorillonite | octahedral/tetrahedral | <0.1 μm | 0.36(1) |
| SWa-1 | nontronite | tetrahedral/octahedral | <1 μm | 0.31(1) |
| SbCa-1 | beidellite | tetrahedral | <1.0 μm | 0.50(1) |
| SbId-1 | beidellite | tetrahedral | <0.1 μm | 0.39(1) |
| Saponite | saponite, trioctahedral | tetrahedral | <2 μm | 0.58(1) |

https://doi.org/10.1346/CCMN.2015.0630102 Published online by Cambridge University Press

Estimates of the molecular weights for each smectite were based on literature compositions.

*ATR-IR experiments*

Infrared spectra (4000−580 $cm^{-1}$) were collected on two Fourier transform instruments (Equinox 55 by Bruker Optics and Nicolet 6700 by Thermo Scientific) equipped with single-reflection diamond ATR accessories (DuraSampl IR II by SensIR Technologies and high-temperature Golden Gate by Thermo Scientific, respectively). The spectra were measured as 100-scan averages with 4 $cm^{-1}$ resolution ($\Delta\nu$ = 2 $cm^{-1}$ by interferogram zerofill) and reported after correction for the dependence of the penetration depth on wavelength. Second derivatives were calculated with Savitzky-Golay routines.

Spectra were measured from ~5−10 μm-thick films. The films were made by careful depositing and drying of a few drops of an aqueous sonicated suspension of smectite on the top of the ATR crystal, avoiding air bubbles or voids that could reduce contact between the thin film and the ATR crystal surface. The ATR plate was fitted with a home-made purging cap which enabled IR monitoring during purge drying or vapor hydration at ambient temperature (25±1ºC). The as-prepared smectite films were subjected to one of the following treatments:

(a) Equilibration under a $N_2$ flow with adjustable relative humidity (RH = 19−90±2%) of $H_2O$ or $D_2O$ vapor, which was produced by a humidity generator (HG-100 by L&C Science and Technology, Hialeah, Florida, USA). At each stepwise stabilized RH value, two spectra were collected after ~5 and ~10 min to ensure sample equilibration with the vapor.

(b) Alternating $D_2O$/HDO/$H_2O$ wetting and $N_2$ purge-drying cycles as in Bukas *et al*. (2013). During each cycle, equilibration for at least 15 min was performed in order to achieve complete substitution.

$N_2$ of purity 5.0 and $D_2O$ with 99.9%$_{at}$, D/H (Sigma-Aldrich) were used in both cases. A systematic study of hydration/dehydration kinetics (*cf.* Fu *et al.*, 1990) was not performed and the quantitative determination of $H_2O$/$D_2O$ in the smectite samples is beyond the scope of this paper.

## RESULTS AND DISCUSSION

*Smectites saturated with $H_2O$ at different RH conditions*

The dependence of the ATR-IR spectra of Ca- and Na-SWy-2 exposed to variable RH (19−90% at 25ºC, Figure 1) is typical for montmorillonite and analogous trends have been reported in numerous previous publications (*e.g.* Xu *et al.*, 2000; Madejová *et al.*, 2002; Madejová, 2003 and references therein). Briefly, IR activity is observed in three frequency ranges: ~3700−3000 $cm^{-1}$ ($\nu$ O−$H_s$, O−$H_w$), 1650−1600 $cm^{-1}$ ($\delta$ $H_2O$), and ~1200−800 $cm^{-1}$ (dominated by various strong Si−O modes). The bending modes of the structural OH groups ($\delta$ $OH_s$) are superimposed on the low-frequency side of the strong Si−O envelope and are diagnostic of the octahedral layer substitutions. In the spectrum of SWy-2 these bending modes are observed at ~915, 881, and 843 $cm^{-1}$ and attributed to $Al_2OH$, AlFe(III)OH, and AlMgOH pairs, respectively (*e.g.* Madejová *et al.*, 2002; Madejová, 2003; Gates, 2005 and references therein). In contrast to the bending modes, the corresponding O−$H_s$ stretching component bands of the three dioctahedral species are not easily resolved (Zviagina *et al.*, 2004 and references therein). These $OH_s$ bands contribute collectively to the band at 3625 $cm^{-1}$ (Figure 1), which appears to be rather insensitive to both the hydration state and the interlayer cation.

The effect of progressively decreasing RH on the spectrum of montmorillonite is largely manifested by the decrease in intensity and slight shift to higher frequencies of the broad peaks at ~3400 $cm^{-1}$. The exact position of this peak is cation dependent (3392 $cm^{-1}$ in Ca-SWy-2 and 3405 $cm^{-1}$ in Na-SWy-2, Figure 1). A less pronounced decrease in intensity of the band at ~1630 $cm^{-1}$ and a concomitant shift to lower frequencies upon drying are observed, in agreement with previous literature (Johnston *et al.*, 1992; Madejová *et al.*, 2002; Madejová, 2003; Gates, 2005). Clearly, the features at ~3400 and ~1630 $cm^{-1}$ ought to be attributed to $H_2O$ on the basis of their response to drying and their dependence on the interlayer cation. A weak shoulder at ~3215 $cm^{-1}$ is also ubiquitous in the spectra of smectites (Figure 1). An early assignment of this feature to the overtone of the $H_2O$ bending (~1630 $cm^{-1}$) by Farmer (1974) has been adopted in the recent literature. Perhaps a more appropriate description would consider the ~3400 and 3215 $cm^{-1}$ bands of $H_2O$ as resulting from the Fermi resonance between the stretching fundamental and the bending overtone of $H_2O$ (Efimov and Naberukhin, 2002; Sovago *et al.*, 2009). Some smectites are reported to exhibit an additional poorly resolved band at 3580−3540 $cm^{-1}$, also attributed to O−$H_w$ stretching (Bishop *et al.*, 1994; Xu *et al.*, 2000; Madejová *et al.*, 2002) and not to O−$H_s$ (*e.g.* Zviagina *et al.*, 2004). All typical $H_2O$-related features and trends upon drying were observed for all smectites in this study. Comparing the Ca- and Na-forms of the SCa-3 montmorillonite and the SbCa-1 beidellite (Figure 2) with those of SWy-2 (Figure 1) indicated that each smectite responds to changing %RH by adjusting the intensity of the broad band at ~3400 $cm^{-1}$, whereas the high-frequency sharp O−H stretching component is relatively unaffected. The position of the ~3400 $cm^{-1}$ band appeared to depend more on the type of interlayer cation and less on the type of 2:1 layer. The ~3400 $cm^{-1}$ band shifted to higher frequencies upon drying and this effect was more pronounced in the Na- than in the Ca-smectites (Figure 3a). This is mostly because, for any given value of %RH, the $H_2O$ content of smectites is strongly dependent on the nature of the interlayer cation.

https://doi.org/10.1346/CCMN.2015.0630102 Published online by Cambridge University Press

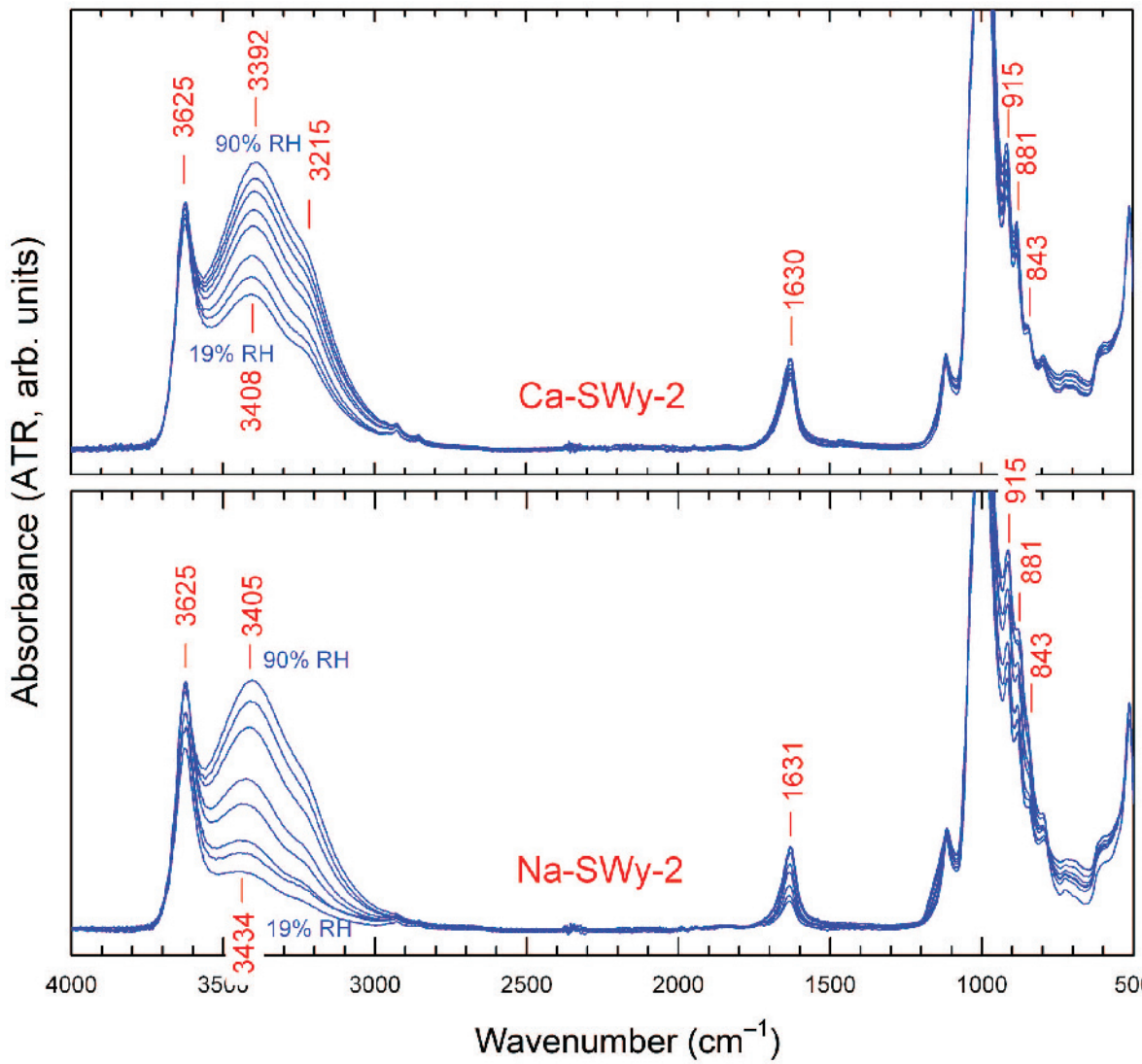


Figure 1. ATR-IR spectra of Ca- (upper) and Na-SWy-2 montmorillonite (lower) as a function of relative humidity (19−90%) at 25ºC.

According to Chiou and Rutherford (1997), Ca-SWy-1 equilibrated at 90% RH has ~250 mg of $H_2O$/g clay whereas the corresponding content in Na-SWy-1 is ~190 mg $H_2O$/g. Similarly, at 19% RH the $H_2O$ contents are ~90 mg of $H_2O$/g in Ca-SWy-1 and 15 mg of $H_2O$/g in Na-SWy-1 corresponding to 10.4 and 0.9 $H_2O$ molecules per exchangeable cation, respectively. These trends in $H_2O$ content *vs.* %RH were in qualitative agreement not only with the varying intensity of the 3500−3000 cm$^{-1}$ envelope (Figures 1 and 2) but also with its varying position (Figure 3b), in agreement with Xu *et al.* (2000) and Madejová *et al.* (2002). In contrast, changes in the water content appeared not to affect the position, intensity, and shape of the ~3625 cm$^{-1}$ band, which was least sensitive to the interlayer cation type and hydration stage in the range of water content studied (Figures 1 and 2). As shown by Madejová *et al.* (1994) and Zviagina *et al.* (2004), the exact position (3633 cm$^{-1}$ in SbCa-1, 3625 cm$^{-1}$ in SWy-2, and 3616 cm$^{-1}$ in SCa-3 in both the Ca- and Na-series) and the shape of the ~3625 cm$^{-1}$ band in the three smectites are related to their different octahedral-sheet compositions.

Based on the information above, the response of the smectite IR spectra to varying hydration appears to be consistent with the assignments of the ~3625 cm$^{-1}$ and ~3400 cm$^{-1}$ bands to O−H$_s$ (structural) and O−H$_w$ (water), respectively, in agreement with many recent studies (Xu *et al.*, 2000; Madejová and Komadel, 2001; Madejová *et al.*, 2002; Madejová, 2003). Does this simple interpretation withstand a $D_2O$ saturation test? $D_2O$ saturation is expected to move the entire set of $H_2O$ bands to lower frequencies, replacing the δ $H_2O$ at ~1630 cm$^{-1}$, its overtone at ~3215 cm$^{-1}$, and the

https://doi.org/10.1346/CCMN.2015.0630102 Published online by Cambridge University Press

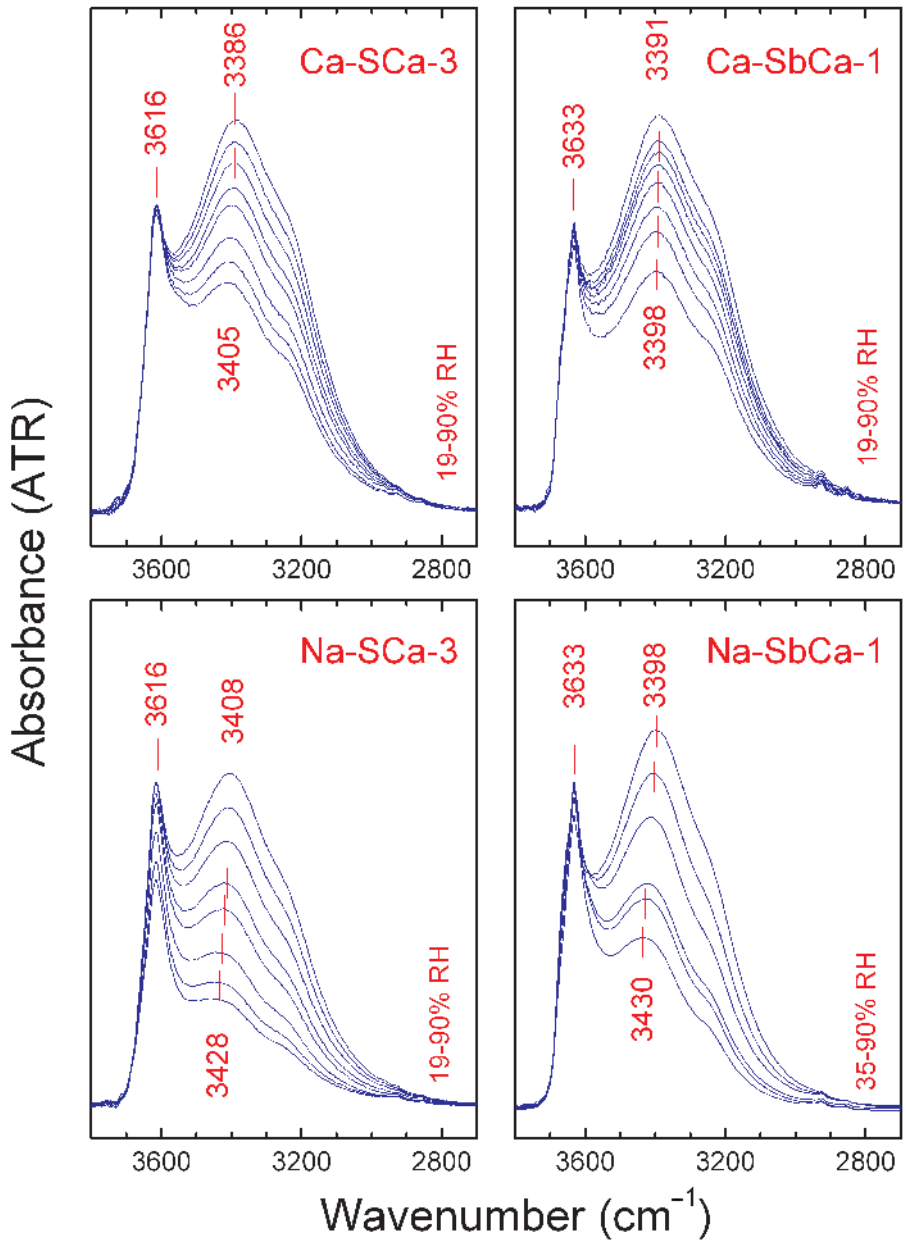


Figure 2. Details of the ATR-IR spectra of Ca- and NaSCa-3 montmorillonite and high-charge beidellite (SbCa-1) as a function of relative humidity at 25ºC.

ν O–$H_w$ at ~3400 $cm^{-1}$ with their corresponding $D_2O$ bands at ~1200, ~2370, and ~2500 $cm^{-1}$, respectively (ν (H/D) ≈ 1.36). If the three aforementioned $H_2O$ bands are the only ones that originate from water adsorbed on the smectite surface, no new bands other than their $D_2O$ analogs should be observed upon $D_2O$ saturation.

*$D_2O$- vs. $H_2O$-saturated samples*

Cycling $D_2O$ vapors and dry $N_2$ at ambient conditions over oriented smectite film resulted in an almost complete saturation with $D_2O$, as indicated by the comparison of the ATR-IR spectra of the $H_2O$- and $D_2O$-forms of Na-SWy-2 (Figure 4), collected at ~50% RH (*cf.* Figure 3). The 1200–800 $cm^{-1}$ range of a smectite spectrum undergoes systematic changes in peak positions and intensities upon varying %RH (in agreement with Yan *et al.*, 1996), regardless of whether the sample is saturated with $D_2O$ or $H_2O$. Appropriate comparison of data collected during different experiments (*e.g.* Figure 4) required, therefore, that the spectra be matched based on the same or very similar hydration states.

Saturation with $D_2O$ resulted in a significant decrease in absorbance at 3800–3000 $cm^{-1}$ (due to O–$H_w$ stretching)

https://doi.org/10.1346/CCMN.2015.0630102 Published online by Cambridge University Press

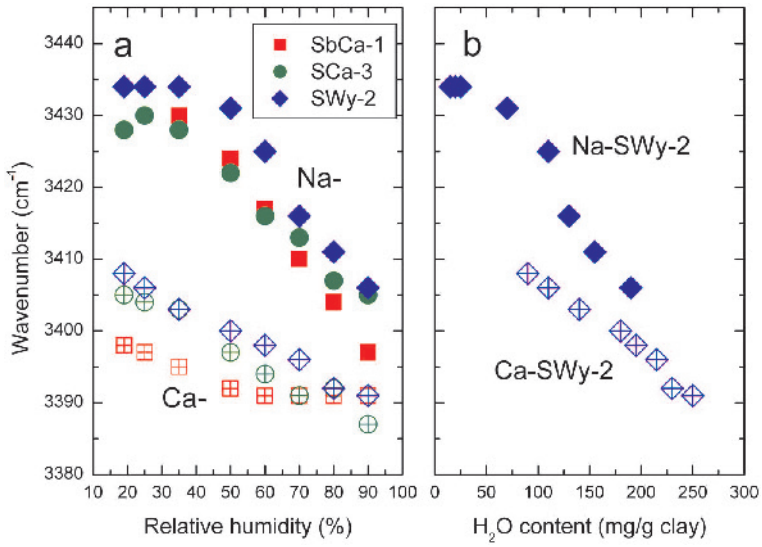


Figure 3. (a) Dependence of the position of the $H_2O$ stretching mode at ~3400 cm$^{-1}$ on relative humidity for the clays shown in Figures 1 and 2. (b) The same frequency data for SWy-2 plotted *vs.* the corresponding $H_2O$ contents of Chiou and Rutherford (1997).

and the appearance of a new complex band envelope of O–D stretching at 2800–2200 cm$^{-1}$. A sharp, asymmetric O–H band peaking at 3624 cm$^{-1}$ persisted during $D_2O$ saturation at ambient conditions. A spectral difference profile between $D_2O$- and $H_2O$-saturated forms of Na-SWy-2 (Figure 4) is close in shape to the O–D profile, but the positions of bands are shifted by ν (H/D) = 1.36. Furthermore, the bending mode of $D_2O$ was observed at ~1205 cm$^{-1}$, no $H_2O$ bending was observed at ~1630 cm$^{-1}$, and the very low-intensity band at ~1450 cm$^{-1}$ indicated that there was no significant contribution from HDO molecules. The 2δ $D_2O$ Fermi-resonant overtone was also noticeable at 2374 cm$^{-1}$, as anticipated.

The as-produced O–D stretching profile of $D_2O$-saturated Na-SWy-2 exhibited the expected broad features of liquid $D_2O$ peaking at ~2500 cm$^{-1}$ (Bertie *et al.*, 1989), but involved an additional sharp feature observed at 2686 cm$^{-1}$ in the absorbance mode, which was better resolved at 2692 cm$^{-1}$ in the 2$^{nd}$ derivative mode (Figure 4). The corresponding O–H position was 3638 cm$^{-1}$ (H/D = 1.35), as determined from the 2$^{nd}$ derivative of the $H_2O$–$D_2O$ difference spectrum.

The origin of the sharp 2692 (3638) cm$^{-1}$ O–D (O–H) band needs to be clarified. A close inspection of both absorbance and the 2$^{nd}$ derivative spectra of $H_2O$- and $D_2O$-wet Na-SWy-2 (Figure 4) indicated that the intensity of the δ OH bands (at 913, 878, and 841 cm$^{-1}$, respectively) did not decrease upon $D_2O$ wetting and no features attributable to δ $OD_s$ were observed. Hence, the $D_2O$ saturation under the conditions employed did not produce $OD_s$ detectable by IR. As a consequence, the sharp 2692 (3638) cm$^{-1}$ band ought to be associated with $OD_w$ ($OH_w$). The presence of this sharp high-frequency $D_2O$ band, which is absent from the spectra of liquid $D_2O$ (Max and Chapados, 2009), is ubiquitous in the spectra of all smectites and in all cationic forms investigated here. Several representative examples (Figure 5) demonstrate that the 3800–2800 cm$^{-1}$ spectral difference between the $H_2O$- and $D_2O$-saturated samples matches in all cases the 2800–2100 cm$^{-1}$ O–D stretching envelope of $D_2O$. In most $H_2O$-wet samples, the frequency range between 3650 and 3615 cm$^{-1}$ involves unresolved contributions from both O–$H_w$ and O–$H_s$. Exceptions are saponite and nontronite which exhibit O–$H_s$ modes at higher and lower frequencies, respectively ($Mg_3OH$: ~3683 cm$^{-1}$, $Fe(III)_2OH$: ~3560 cm$^{-1}$). Incidentally, the fact that $D_2O$-wet saponite and nontronite both exhibit a high-frequency $D_2O$ stretching peak differing by <30 cm$^{-1}$ (Figure 5) whereas their structural $OH_s$ peaks are >120 cm$^{-1}$ apart adds further support to the assignment of the high-frequency O–D stretching to O–$D_w$ and not to O–$D_s$.

Further evidence supporting the assignment of the sharp 2692 (3638) cm$^{-1}$ band to O–$D_w$ (O–$H_w$) comes from the near-IR spectra of smectites, which allow for the full separation of $OH_w$ from $OH_s$ by means of the (ν+δ) stretching-bending combination modes, due to large separation between the combination modes of smectite structure (ν O–$H_s$ ~3620 cm$^{-1}$, δ $OH_s$ ~916 m$^{-1}$ and below that results in (ν+δ) at ~4536 cm$^{-1}$) and water (ν O–$H_w$ ⩾3610 m$^{-1}$, δ $H_2O$ at ~1635 m$^{-1}$ which results in (ν+δ) at ~5250 cm$^{-1}$) (Bishop *et al.*, 1994; Cariati *et al.*, 1981). Montmorillonite clays exhibit a sharp $H_2O$ (ν+δ) combination mode at ~5250 cm$^{-1}$ (Clark *et al.*, 1990; Bishop *et al.*, 1994). As the position of δ ($H_2O$) is always at ~1630 cm$^{-1}$, analogous to δ ($D_2O$) at ~1205 cm$^{-1}$ (Table 2), the (ν+δ) combination band cannot possibly involve the stretching at ~3420 cm$^{-1}$ and requires the presence of a ν (O–$H_w$) mode with a position greater than 3610 cm$^{-1}$ (Cariati *et al.*, 1981).

Based on the above, the sharp band at 2680–2694 cm$^{-1}$, which is observed in all $D_2O$-wet

https://doi.org/10.1346/CCMN.2015.0630102 Published online by Cambridge University Press

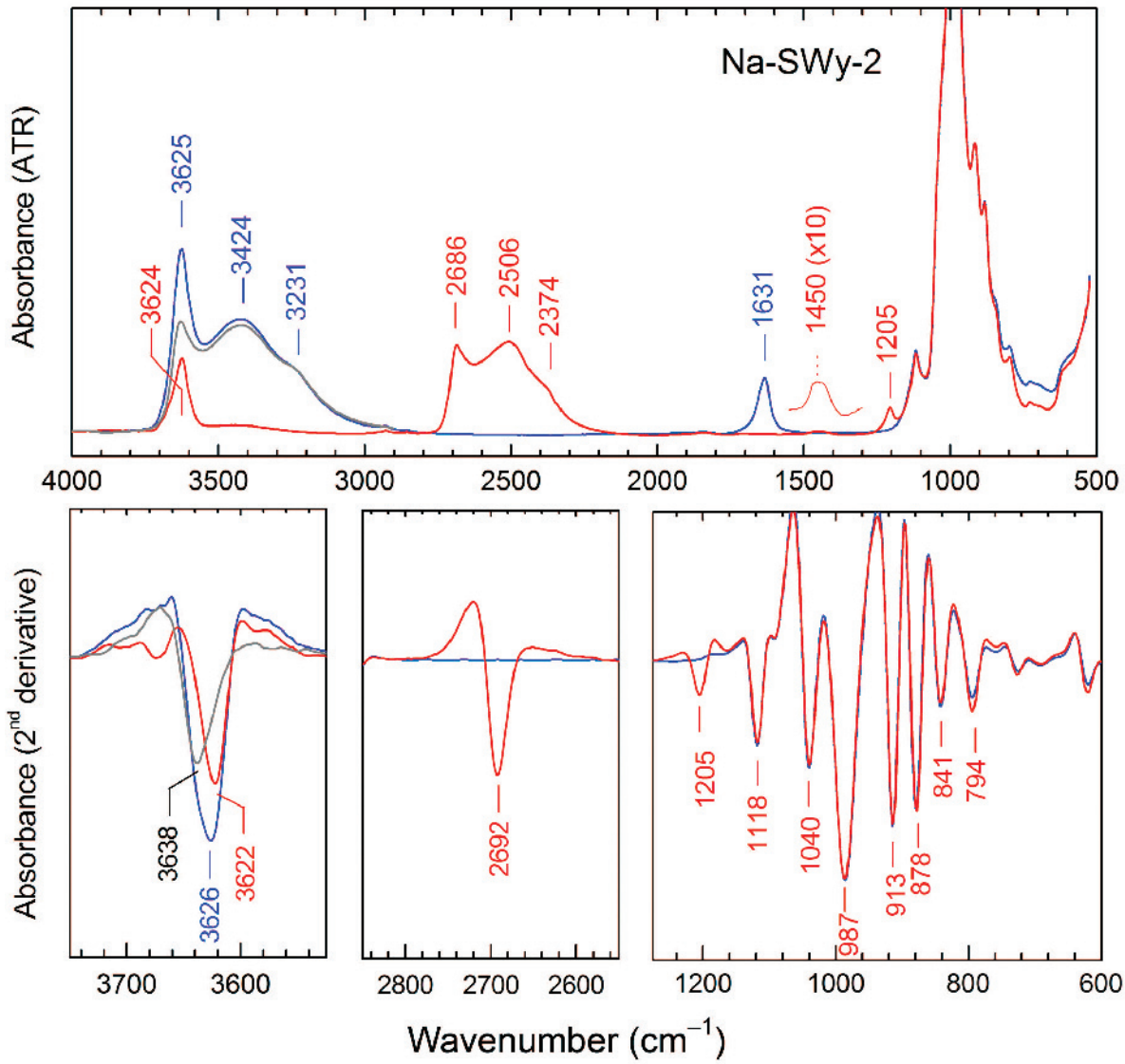


Figure 4. (Upper) Comparison of the ATR-IR spectra of Na-SWy-2 montmorillonite equilibrated by $H_2O$ (blue) and $D_2O$ (red) at ~50% relative humidity, 25ºC. Their difference spectrum in the 4000–2800 $cm^{-1}$ range is included (gray). The very weak absorbance intensity at ~1450 $cm^{-1}$ indicates that only trace HDO is present in the $D_2O$ sample. (Lower) Details of the 2nd derivative ATR-IR and difference spectra over selected wavenumber ranges.

Table 2. Positions ($cm^{-1}$) of the high-energy O–D stretching component, ν (O–D), and bending δ ($D_2O$) bands for $D_2O$-saturated samples at ambient conditions and in different cationic forms. Band positions were determined from the minima of 2nd derivatives with 13-point Savitzky Golay smoothing.

| Sample name | ν (O–D) | | | δ ($D_2O$) | | |
|---|---|---|---|---|---|---|
| | Ca | Na | Cs | Ca | Na | Cs |
| SWa-1 | 2692.1(5) | 2692.8(5) | 2691.4(1) | 1202.3(5) | 1202.6(5) | 1203.8(5) |
| SWy-2 | 2691.7(5) | 2692.1(5) | 2693.2(5) | 1201.9(5) | 1203.6(5) | 1207.1(5) |
| SbId-1 | 2689.3(5) | 2689.4(5) | 2691.6(5) | 1203.8(5) | 1205.0(5) | 1207.6(5) |
| SbCa-1 | 2685.5(5) | 2684.5(5) | n.a. | 1204.9(5) | 1207.4(5) | n.a. |
| SCa-3 | 2686.2(5) | 2685.5(5) | 2689.4(5) | 1202.4(5) | 1204.9(5) | 1206.5(5) |
| SAz-2 | 2686.0(5) | 2686.1(5) | 2690.0(5) | 1202.4(5) | 1204.9(5) | 1206.2(5) |
| SAP | 2684(2) | 2682(2) | 2687(2) | 1204.4(5) | 1205.5(5) | 1205.0(5) |

https://doi.org/10.1346/CCMN.2015.0630102 Published online by Cambridge University Press

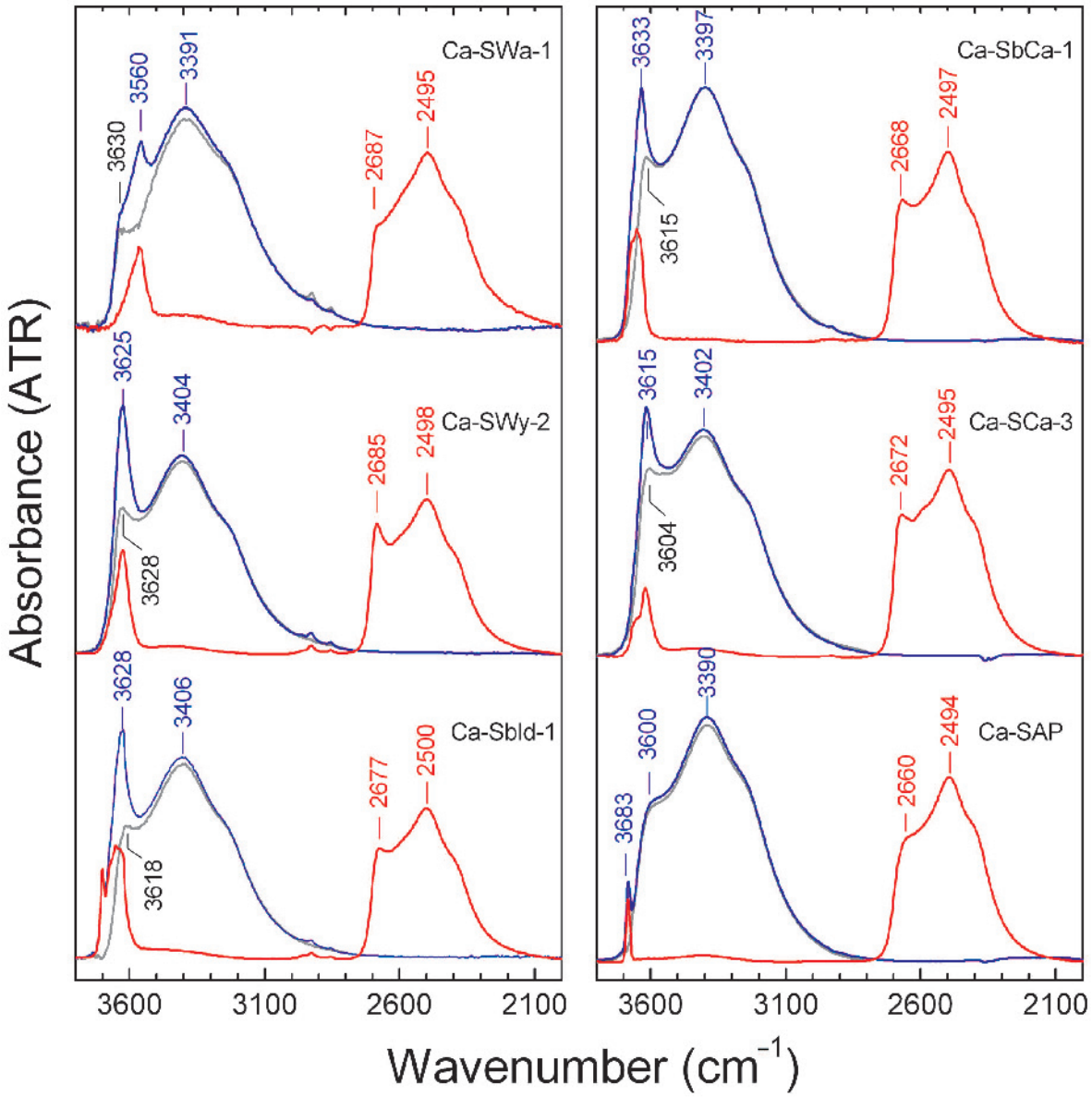


Figure 5. Absorbance spectra of smectites equilibrated with ~50% RH of $H_2O$ (blue) or $D_2O$-vapor (red) and their difference in the O−H stretching range (gray). The spectra of the SAz-2 montmorillonite (SAz-2, not shown) are nearly identical to those of the SCa-3 sample. All samples are in Ca-form.

smectites, must be produced by a $D_2O$ stretching mode and not by deuterated structural hydroxyls. In $H_2O$-wet samples, this band has an analog at 3638 cm$^{-1}$ which cannot be resolved easily from the stretching modes of the structural hydroxyl groups (O−$H_s$) peaking at ~3622 cm$^{-1}$ (Figure 4).

*Smectites saturated with $D_2O$ at different RH conditions*

In the O−D stretching region, the intensity of a band at ~2500 cm$^{-1}$ increased with increasing %RH, as shown for a representative sample SWy-2 (Figure 6), irrespective of interlayer cation type. This trend is similar to the evolution of the $OH_w$ stretching envelope (*cf.* Figures 1 and 6). The sharp band at ~2686 cm$^{-1}$ is always present in the spectra, irrespective of %RH, with a relatively uniform intensity for the Ca-form, except at the lowest %RH values. The number of $D_2O$ molecules responsible for the sharp band must thus remain relatively constant throughout the experiment, whereas the number of molecules in the non-interface position in the interlayer (cation-bound, bulk water) decreases with decreasing RH, causing a significant intensity decrease below 2600 cm$^{-1}$ (*cf.* Johnston *et al.*, 1992; Xu *et al.*, 2000). The same trend is visible for Na-SWy-2 although changes in the position and intensity of the sharp band are more pronounced and start at higher RH (Figure 6).

https://doi.org/10.1346/CCMN.2015.0630102 Published online by Cambridge University Press

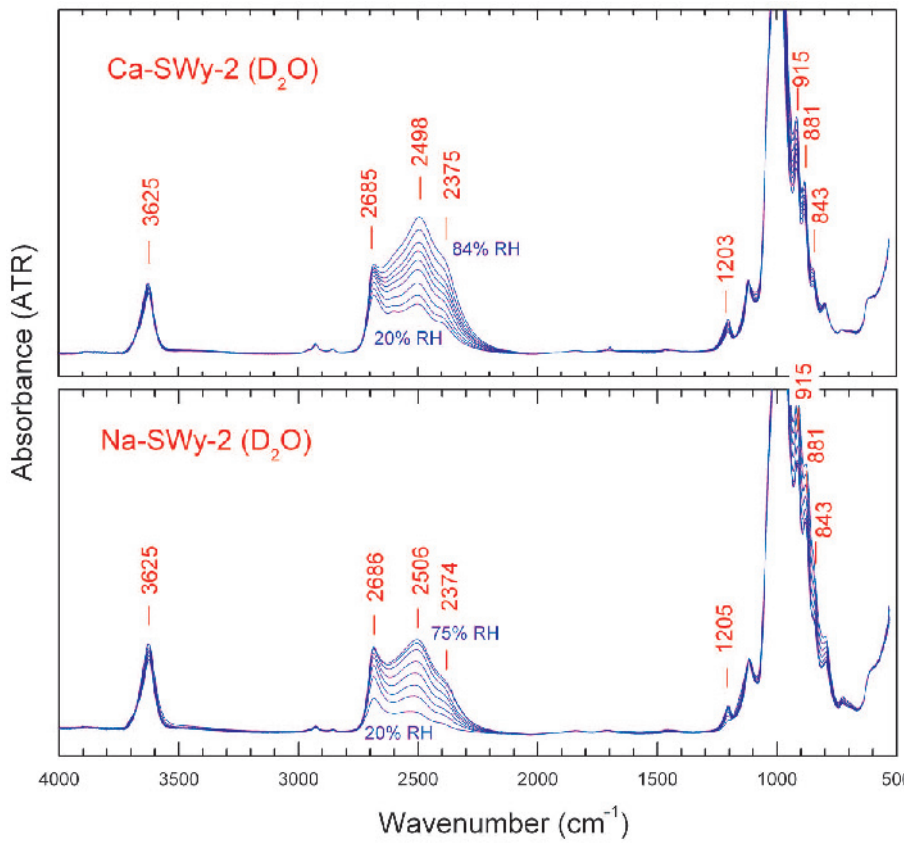


Figure 6. ATR-IR spectra of $D_2O$-exchanged, Ca- (upper) and Na-SWy-2 montmorillonite (lower) equilibrated at variable $D_2O$ relative humidity at 25ºC.

The lack of structural O–$D_s$ bending bands at frequencies observed by Russell *et al.* (1970) proves that, within the detection limits of ATR-IR, no deuteration of structural OH groups occurred.

Changes of the sharp band position as a function of changing RH were traced with a 2nd derivative approach for samples SWy-2 and SCa-3 in Na- and Ca-forms (Figure 7). The sharp band is at higher frequency for SWy-2 in both cationic forms than for the SCa-3 sample and is relatively constant for RH between 60 and 80%. At lower RH, the frequency of the sharp band decreases. The band position for the SCa-3 sample stays relatively constant across a broad range of RH for both interlayer cations (Figure 7). The largest difference in the sharp band position between the samples is observed for RH between 60 and 80%. In all samples studied the sharp band position is very stable within that range of RH. The RH range between 60 and 80% was, therefore, chosen to

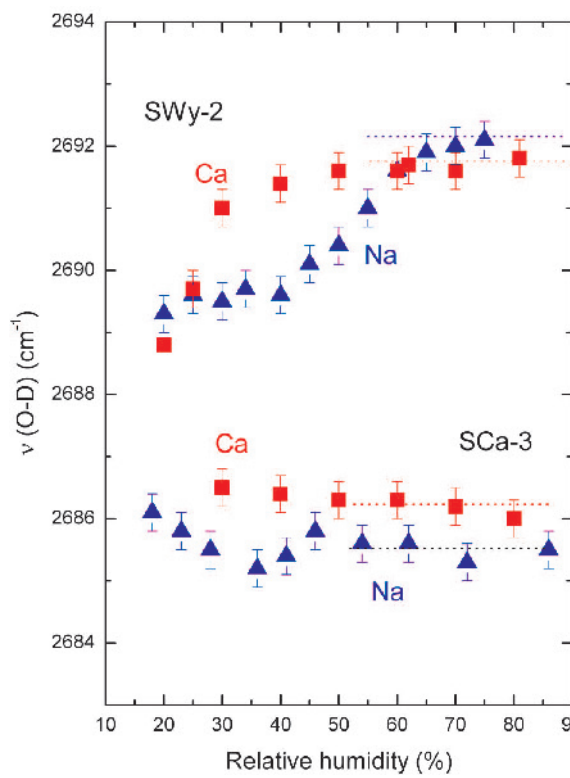


Figure 7. Positions ($cm^{-1}$) of the high-frequency O–D stretching component, ν (O–D), of $D_2O$-saturated SWy-2 and SCa-3 montmorillonite in Ca- and Na-forms as a function of $D_2O$ relative humidity at 25ºC. Values are taken from the minima of the 2nd derivatives with 13-point Savitzky Golay smoothing. Dashed lines indicate average values included in Table 1.

https://doi.org/10.1346/CCMN.2015.0630102 Published online by Cambridge University Press

record the sharp band positions for the remaining samples, despite greater overlap with a broad O–D stretching band at ~2500 $cm^{-1}$.

*Systematics of the high-frequency $D_2O$ stretching band in smectites*

A 2nd derivative with 13-point Savitzky-Golay filter, corresponding to a window of ±12 $cm^{-1}$ around the central point, was employed to find the peak position of the sharp band for each smectite analyzed (Table 2). This smoothing filter was chosen to provide the maximum contrast between the sharp 2700–2670 $cm^{-1}$ O–D stretching band and the broader 2500– and 2400 $cm^{-1}$ component band. The 2nd derivative minima of the O–D bands were consistently found at higher energy than the apparent maxima of the corresponding absorbance spectra (*e.g.* Figure 4), which can be explained by the presence of additional poorly resolved components in the 2700–2500 $cm^{-1}$ range that results in the shifting of the apparent absorbance maxima towards slightly lower frequency.

A linear decrease of frequency was observed upon increasing the total layer charge of the smectite (Table 2 and Figure 8). No effects of octahedral layer type (dioctahedral or trioctahedral) or charge location (tetrahedral or octahedral) on peak position were observed. In addition, little or no difference between the Ca-saturated and Na-saturated smectite series was noted. The fitted lines for Ca- and Na-saturated smectites (Figure 8) were identical within error and could be approximated by a single equation:

$$\nu\ (O–D) = 2703.9 - 35.8Q_{tot},\ (R^2 = 0.94,\ n = 14) \quad (1)$$

The Cs-saturated series showed a much weaker dependence on $Q_{tot}$:

$$\nu\ (O–D) = 2698 - 17Q_{tot},\ (R^2 = 0.76,\ n = 6) \quad (2)$$

*HDO-saturated smectites*

The stretching envelope of $H_2O$ and $D_2O$ is complicated by the intramolecular coupling between the two O–H or two O–D bonds. In an attempt to reduce this intramolecular coupling, some earlier studies (*e.g.* Farmer and Russell, 1971; Suquet *et al.*, 1977) reported the spectra of HDO instead of $D_2O$ in smectites. Briefly, this type of isotopic enrichment involves wetting the samples with a mixture of $D_2O$:$H_2O$, typically 20:80 by volume (~36% HDO, 60% $H_2O$, and 4% $D_2O$), and

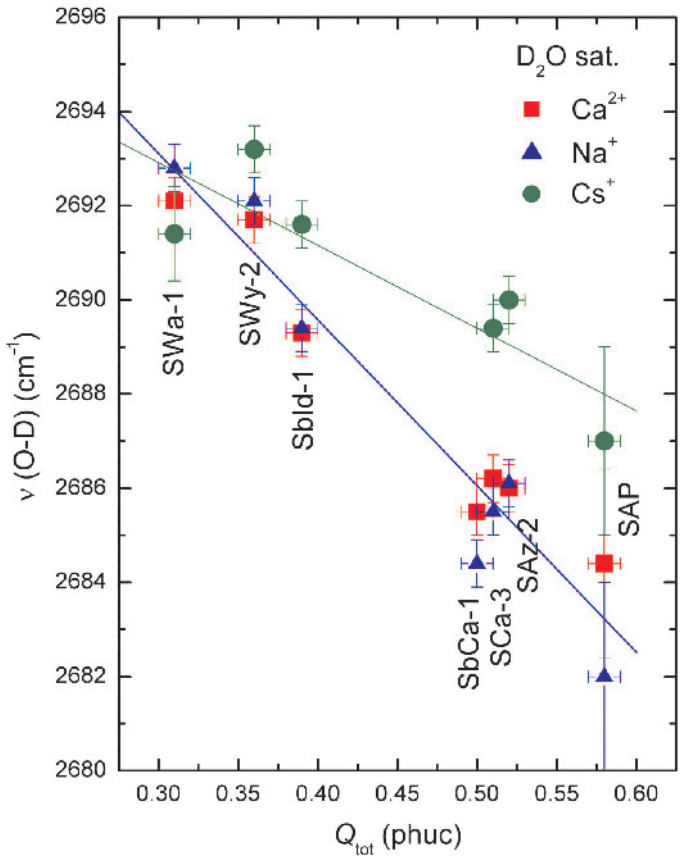


Figure 8. Dependence of the position of the sharp, high-frequency O–D stretching of $D_2O$-saturated smectites on total charge per half unit cell ($Q_{tot}$) and compensating cation ($Ca^{2+}$, $Na^+$ and $Cs^+$). The straight lines are least-squares fits.

https://doi.org/10.1346/CCMN.2015.0630102 Published online by Cambridge University Press

studying the spectra in the O–D stretching range (Figure 9). The HDO-saturation experiments of all seven smectites in three cation forms were performed. The sharp, high-energy OD band of HDO was observed in all samples, always at wavelengths 20–30 $cm^{-1}$ lower than in $D_2O$-saturated samples, in qualitative agreement with Farmer and Russell (1971). A similar dependence on smectite charge and interlayer cation was observed as in the case of $D_2O$-wetting (Figure 10). In contrast, the strongly H-bonded part of the $D_2O$ stretching domain showed an opposite shift (2506 for $D_2O$ and 2523 $cm^{-1}$ for HDO in the case of Na-SWy-2 – Figure 9). In addition, the ~2400 $cm^{-1}$ component was absent from the spectra of the HDO-smectite, which is consistent with its assignment to a Fermi resonance 2δ $D_2O$ component and simplifies the spectrum of HO–D stretching modes. On the other hand, the advantages of studying HDO- instead of $D_2O$-saturated smectite samples are counterbalanced by the inevitably weaker intensity of the HO–D stretching envelope, which results in a worse signal-to-noise ratio and the larger bandwidths associated with the isotope combinations in a mixed H-bonded tetrahedral $O(H,D)_4$ network (Max and Chapados, 2002).

*Origin of the sharp $O–D_w/O–H_w$ band*

Within the %RH range studied, the sharp, high-frequency IR band at ~2685 $cm^{-1}$ ($D_2O$) or ~3630 $cm^{-1}$ ($H_2O$) was a common feature for all smectites investigated, with a position and intensity showing remarkable insensitivity to interlayer cation type or interlayer water content, but with noticeable dependence on layer charge (Table 2, Figure 5). An opposite behavior was observed for the ~3400 $cm^{-1}$ ($H_2O$), and ~2500 $cm^{-1}$ ($D_2O$) $OH_w/OD_w$ stretching envelopes that exhibited a strong dependence on hydration stage and interlayer cation (*cf.* Xu *et al.*, 2000; Madejová *et al.*, 2002), but were relatively unaffected by the layer charge or charge location of the smectites studied (Figure 4).

Notably, the position of the sharp band showed a negligible difference between the Na- and Ca-forms of any of the smectites studied, despite the large difference in ionic potential and hydration enthalpy between these cations. $Cs^+$ has the lowest hydration enthalpy among naturally occurring single, non-complex cations. Nevertheless, Cs-smectites obey a weak linear relationship between the OD sharp band position and the total layer charge of smectite although the correlation line slope is different from the Na- and Ca-forms.

The high frequency of the sharp stretching mode suggests its origin from O–H (O–D) oscillators which are involved in very weak or no H-bonding, unlike liquid water and most aqueous ionic salt solutions (Max *et al.*, 2007). According to Libowitzky (1999), O–H stretching frequencies in silicate minerals which are in excess of 3600 $cm^{-1}$ correspond to O···O distances >~3.1–3.2 Å. In contrast to this estimated distance, the average O···O distance of liquid $H_2O$ is ~2.8 Å, while the common perception of the H bond corresponds to O···O distances of <~3.1 Å (Khan, 2000). Lastly, the nearly constant intensity of the high-frequency band over broad ranges of water content indicates that the $H_2O$ species responsible for this band is not sensitive to the actual expansion of the interlayer which does depend on water content (*cf.* Ferrage *et al.*, 2010). The origin of the sharp band from the water interface on the siloxane surface seems, therefore, the only valid mechanism, because its occurrence, position, and – on a qualitatively observable level – its intensity do not depend directly on the interlayer cation; neither does the band represent the bulk of the interlayer water.

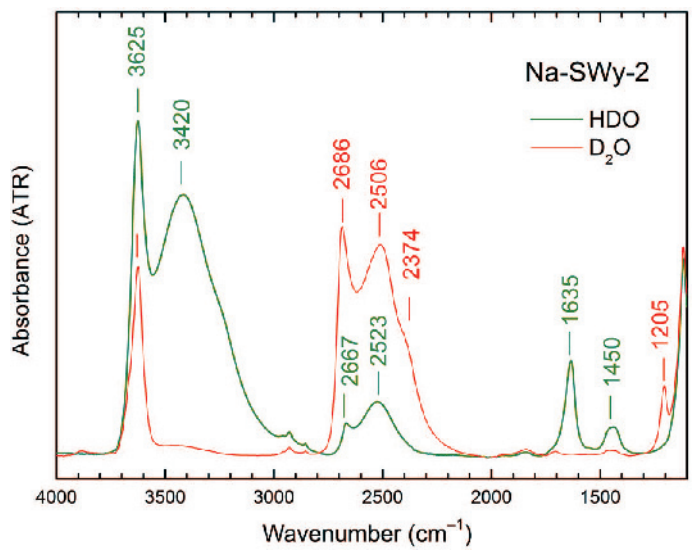


Figure 9. Comparison of the ATR-IR spectra of HDO- and $D_2O$-saturated Na-SWy-2 montmorillonite.

https://doi.org/10.1346/CCMN.2015.0630102 Published online by Cambridge University Press

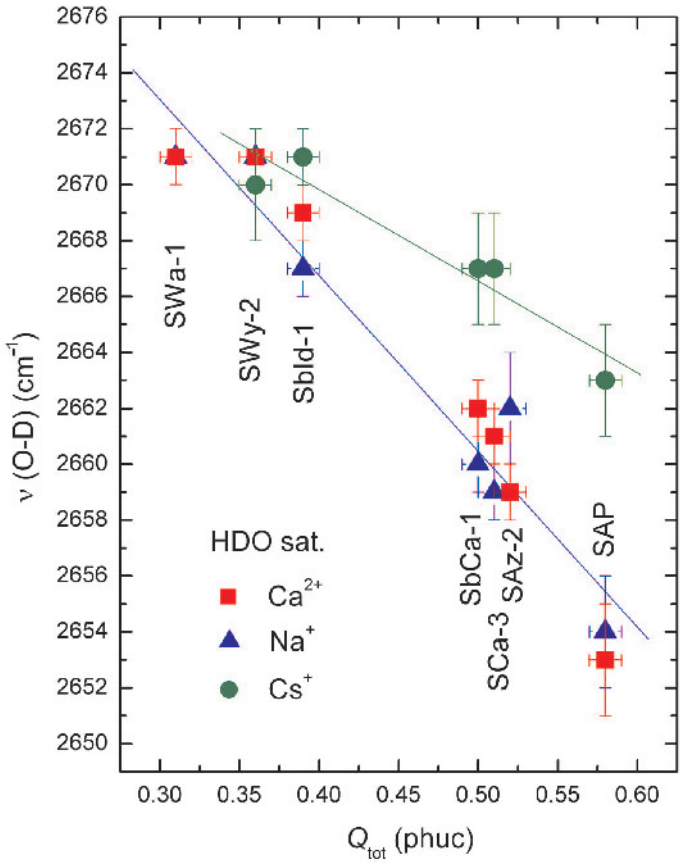


Figure 10. Same as Figure 8, based on HDO-saturated smectites.

O–H stretching bands at frequencies similar to or even greater than those reported here have been observed at the interface of $H_2O$ with hydrophobic solids (*e.g.* silica, Jena and Hore, 2010) or liquids (*e.g.* $CCl_4$, Scatena *et al.*, 2001), or at the water–vapor interface (Sovago *et al.*, 2009; Tian and Shen, 2009) and are interpreted as modes of so-called 'dangling' OH (Shen and Ostroverkhov, 2006; Auer and Skinner, 2009; Sovago *et al.*, 2009; Tian and Shen, 2009; Zhang *et al.*, 2009; Chakraborty and Chandra, 2012; Davis *et al.*, 2012), *i.e.* vibration of OH groups that are involved in only very weak or non-existent interactions with other atoms. Notably, the siloxane surface of smectite is classified as mostly hydrophobic, based on aromatic-hydrocarbon adsorption experiments (Jaynes and Boyd, 1991).

In contrast, hydrophilic silica with surface SiOH and $SiO^-$ groups exhibits no high-frequency component of the adsorbed water, as was shown using sum frequency vibrational spectroscopy (Shen and Ostroverkhov, 2006). After making the silica surface hydrophobic by coating it with organic molecules, the sharp, high-frequency band appeared (Shen and Ostroverkhov, 2006; Zhang *et al.*, 2009). Increasing the silica-surface hydrophobicity increased the intensity of the band and shifted the position of the band to higher frequencies (Zhang *et al.*, 2009).

The interpretation presented here is in accord with the conclusions of several early experimental studies on water–smectite interactions (*e.g.* Russell and Farmer, 1964; Farmer and Russell, 1971; Suquet *et al.*, 1977; Sposito and Prost, 1982; Sposito *et al.*, 1983) which identified the high-frequency $OH_w$ band and linked it to $H_2O$ molecules at the surface of the interlayer, pointing one of their O–H bonds towards the siloxane surface ('dangling') and the other towards the 'bulk' interlayer. Further support for this interpretation comes from theoretical studies of smectite hydration. Spatial arrangement of $H_2O$ molecules with one or two OH directed toward the siloxane surface was proposed by the theoretical calculations of Prost and Chaussidon (1969) and the molecular dynamics simulations of Sposito *et al.* (1999), Suzuki and Kawamura (2004), Wang *et al.* (2005), and Marry *et al.* (2008).

Based on the considerations above, the high-frequency water OH(OD) stretching band is associated with water molecules at the interface with the siloxane sheet and with at least one OH(OD) group pointing toward the surface, *i.e.* in weak interaction with its siloxane O atoms and with negligible influence by interlayer

https://doi.org/10.1346/CCMN.2015.0630102 Published online by Cambridge University Press

cations. Indeed, within the resolution of the experiments performed, the only dependence of this band on the type of smectite was a small decrease in its frequency upon increasing layer charge. The observed shift of the band position was consistent with the development of some attractive interactions between the hydroxyl group of water and the increasingly charged 2:1 layer which would reduce the vibrational frequency of the dangling hydroxyl group. If confirmed on a large set of smectites, the high-frequency $OH(D)_w$ band may become a probe to measure the total layer charge of smectite.

## CONCLUSIONS

The present study has provided new evidence in support of an old, sometimes forgotten idea about the structure of $H_2O$ molecules in the interlayer space of smectite minerals. A population of $H_2O$ located in the immediate vicinity of the siloxane surface and interacting very weakly with it has been identified by the ubiquitous presence of a high-frequency, sharp $H_2O$ ($D_2O$) band at ~3630 $cm^{-1}$ (2685 $cm^{-1}$). In dioctahedral aluminous smectites, this band nearly coincides with the stretching modes of the structural OH groups which may explain why it has not been identified in some studies as an $H_2O$ vibration. The IR investigation of $D_2O$-saturated smectites, instead of the commonly studied $H_2O$ analogs, re-emerges, therefore, as a valuable tool for the investigation of bands originating from both water molecules and structural OH groups, and free of the problematic overlap.

In agreement with early IR studies and recent studies of water at interfaces, the sharp, high-frequency $H_2O$ ($D_2O$) band is assigned to O–H pointing away from the 'bulk' interlayer and toward the siloxane surface. The position of this band is nearly independent of the cation ($Na^+$, $Ca^{2+}$) and its intensity remained constant over broad hydration ranges, such as those achieved with 60–80% relative humidity at ambient temperature. A linear dependence of the sharp band position on the total layer charge of a smectite was found. Based on this dependence, it appears that the total layer charge, $Q_{tot}$, can be estimated from the position of the high-frequency O–$D_w$ stretching band with an uncertainty of the order of ±0.03 $e^-$/half unit cell in Na- or Ca-smectites. This preliminary correlation is very promising and requires more data to confirm the trend. The relationship should be checked for the possible presence of systematics specific to octahedral structure (trioctahedral *vs*. dioctahedral, *cis*-vacant *vs*. *trans*-vacant) or charge location (octahedral *vs*. tetrahedral). A caveat that needs to be emphasized is that the exact position of the high-frequency $OD_w$ depends on whether it is determined from maxima in absorbance spectra or minima in the 2nd derivative spectra. A 2nd derivative pre-processing of the spectra is recommended to improve the resolution of the sharp peak against the overlapping broad liquid-like band envelope. A calibration transfer may, therefore, be needed if the peak-picking algorithm is different from that employed in this work.

Finally, the identification of the $OH_w$ contribution to the ~3620 $cm^{-1}$ band of dioctahedral aluminous smectites is essential in assigning correctly the sharp ~5230 $cm^{-1}$ near-IR feature (Cariati *et al.*, 1981, 1983) to a (ν+δ) stretching-bending combination of $H_2O$ in smectites. The sharp band combination mode is particularly intense in the near-IR due to the effect of H-bonding on the anharmonicity of the O–H stretch (Sándorfy, 2006). This opens up the possibility of obtaining similar layer-charge diagnostics from the systematics of the (ν+δ) $OH_w$ combination of $H_2O$ in smectites using the near-IR, more conveniently and without the need for $D_2O$ saturation of samples.

## ACKNOWLEDGMENTS

The authors thank the editors and reviewers for valuable suggestions that helped to improve the manuscript. They are also grateful to Jarosław Kieć for technical assistance. This project was made possible with financial support from project REGPOT-2011-1 under the European Union 7th Framework Programme, No 285989 (ATLAB) and the IGS-PAS research grant for young scientists "Dehydration of smectites – a FTIR, TG and stable isotopes study". Partial support by project KRHPIS 447963 - Polynano (GSRT, TPCI-NHRF) is also acknowledged. This work was performed to partially fulfill the requirements of a PhD thesis by A. Kuligiewicz.

## REFERENCES

Aurer, B.M. and Skinner, J.L. (2009) Water: Hydrogen bonding and vibrational spectroscopy, in the bulk liquid and at the liquid/vapor interface. *Chemical Physics Letters*, **470**, 13–20.

Bertie, J.E., Ahmed, M.K., and Eysel, H.H. (1989) Infrared intensities of liquids. 5. Optical and dielectric constants, integrated intensities, and dipole moment derivatives of $H_2O$ and $D_2O$ at 22ºC. *Journal of Physical Chemistry*, **93**, 2210–2218.

Besson, G. and Drits, V.A. (1997) Refined relationships between chemical composition of dioctahedral fine-grained mica minerals and their infrared spectra within the OH stretching region. Part I: Identification of the OH stretching bands. *Clays and Clay Minerals*, **45**, 158–169.

Bishop, J.L., Pieters, C.M., and Edwards, J.O. (1994) Infrared spectroscopic analyses in the nature of water in montmorillonite. *Clays and Clay Minerals*, **42**, 702–716.

Bukas, V.J., Tsampodimou, M., Gionis, V., and Chryssikos, G.D. (2013) Synchronous ATR infrared and NIR-spectroscopy investigation of sepiolite upon drying. *Vibrational Spectroscopy*, **68**, 51–60.

Bukka, K., Miller, J.D., and Shabtai, J. (1992) FTIR study of deuterated montmorillonites: Structural features relevant to pillared clay stability. *Clays and Clay Minerals*, **40**, 92–102.

Cariati, F., Erre, L., Micera, G., Piu, P., and Gessa C. (1981) Water molecules and hydroxyl groups in montmorillonites as studied by near infrared spectroscopy. *Clays and Clay Minerals*, **29**, 157–159.

Cariati, F., Erre, L., Micera, G., Piu, P., and Gessa C. (1983) Polarization of water molecules in phyllosilicates in relation to exchange cations as studied by near infrared spectro-

https://doi.org/10.1346/CCMN.2015.0630102 Published online by Cambridge University Press

scopy. *Clays and Clay Minerals*, **31**, 155–157.
Chakraborty, D. and Chandra, A. (2012) A first principles simulation study of fluctuations of hydrogen bonds and vibrational frequencies of water at liquid–vapor interface. *Chemical Physics*, **392**, 96–104.
Chiou, C.T. and Rutherford, D.W. (1997) Effects of exchanged cation and layer charge on the sorption of water and EGME vapors on montmorillonite clays. *Clays and Clay Minerals*, **45**, 867–880.
Clark, R.N., King, T.V.V., Klejwa, M., Swayze, G.A., and Vergo, N. (1990) High spectral resolution reflectance spectroscopy of minerals. *Journal of Geophysical Research*, **95B**, 12653–12680.
Davis, J.G., Gierszal, K.P., Wang, P., and Ben-Amotz, D. (2012) Water structural transformation at molecular hydrophobic interfaces. *Nature*, **491**, 582–585.
Efimov, Y.Y. and Naberhukhin, Y.I. (2002) On the interrelation between frequencies of stretching and bending vibrations in liquid water. *Spectrochimica Acta A*, **58**, 519–524.
Farmer, V.C. (1974) The layer silicates. Pp 331–363 in: *The Infrared Spectra of Minerals* (V.C. Farmer, editor). Monograph **4**, Mineralogical Society, London.
Farmer, V.C and Russell, J.D. (1971) Interlayer complexes in layer silicates: The structure of water in lamellar ionic solutions. *Transactions of the Faraday Society*, **67**, 2737–2749.
Ferrage, E., Lanson, B., Michot, L.J., and Robert, J.-L. (2010) Hydration properties and interlayer organization of water and ions in synthetic Na-smectite with tetrahedral layer charge. Part 1. Results from X-ray diffraction profile modeling. *The Journal of Physical Chemistry C*, **114**, 4515–4526.
Fialips, C.-I., Huo, D., Yan, L., Wu, J. and Stucki, J.W. (2002) Effect of Fe oxidation state on the IR spectra of Garfield nontronite. *American Mineralogist*, **87**, 630–641.
Fu, M.H., Zhang, Z.Z. and Low, P.F. (1990) Changes in the properties of a montmorillonite-water system during the adsorption and desorption of water: Hysteresis. *Clays and Clay Minerals*, **38**, 482–492.
Gates, W. P. (2005) Infrared spectroscopy and the chemistry of dioctahedral smectites. Pp. 126–168 in: *The Application of Vibrational Spectroscopy to Clay Minerals and Layered Double Hydroxides* (J.T. Kloprogge, editor). CMS Workshop Lectures, Vol. **13**, The Clay Minerals Society, Boulder, Colorado, USA.
Jackson, M.L. (1969) Dispersion of soil minerals. Pp. 29–91 in: *Soil Chemical Analysis – Advanced Course*. 2nd edition. Published by the author, Madison, Wisconsin, USA.
Jaynes, W.F. and Boyd, S.A. (1991) Hydrophobicity of siloxane surfaces in smectites as revealed by aromatic hydrocarbon adsorption from water. *Clays and Clay Minerals*, **39**, 428–436.
Jena, C.J. and Hore, D.K. (2010) Water structure at solid surfaces and its implications for biomolecule adsorption. *Physical Chemistry Chemical Physics*, **12**, 14383–14404.
Johnston, C.T., Sposito, G., and Erickson, C. (1992) Vibrational probe studies of water interactions with montmorillonite. *Clays and Clay Minerals*, **40**, 722–730.
Khan A. (2000) A liquid water model: Density variation from supercooled to superheated states, prediction of H-bonds, and temperature limits. *Journal of Physical Chemistry B*, **104**, 11268–11274.
Libowitzky, E. (1999) Correlation of O-H stretching frequencies and O-H···O bond lengths in minerals. *Monatshefte für Chemie*, **130**, 1047–1059.
Madejová, J. (2003) FTIR techniques in clay mineral studies. *Vibrational Spectroscopy*, **31**, 1–10.
Madejová, J. and Komadel, P. (2001) Baseline studies of the Clay Minerals Society Source Clays: Infrared methods. *Clays and Clay Minerals*, **49**, 410–432.
Madejová, J., Komadel, P., and Čičel, B. (1994) Infrared study of octahedral site populations in smectites. *Clay Minerals*, **29**, 319–326.
Madejová, J., Janek, M., Komadel, P., Herbert, H.-J., and Moog, H.C. (2002) FTIR analyses of water in MX-80 bentonite compacted from high salinary salt solution systems. *Applied Clay Science*, **20**, 255–271.
Marry, V., Rotenberg, B., and Turq, P. (2008) Structure and dynamics of water at a clay surface from molecular dynamics simulation. *Physical Chemistry Chemical Physics*, **10**, 4802–4813.
Max, J.-J. and Chapados, C. (2002) Isotope effects in liquid water by infrared spectroscopy. *Journal of Chemical Physics*, **116**, 4626–4642.
Max, J.-J. and Chapados, C. (2009) Isotope effects in liquid water by infrared spectroscopy. III. $H_2O$ and $D_2O$ spectra from 6000 to 0 $cm^{-1}$. *Journal of Chemical Physics*, **131**, 184505, 1–13.
Max, J.-J., Gessinger, V., van Driessche, C., Larouche, P., and Chapados, C. (2007) Infrared spectroscopy of aqueous ionic salt solutions at low concentrations. *Journal of Chemical Physics*, **131**, 184507, 1–14.
Pelletier, M., Michot, L.J., Humbert, B., Barrès, O., d' Espinose de la Caillerie, J.-B., and Robert, J.-L. (2003) Influence of layer charge on the hydroxyl stretching of trioctahedral clay minerals: A vibrational study of synthetic Na- and K-saponites. *American Mineralogist*, **88**, 1801–1808.
Petit, S., Robert, J-L., Decarreau, A., Besson, G., Grauby, O., and Martin, F. (1995) Apport des méthodes spectroscopiques à la caractérisation des phyllosilicates 2:1. *Bulletin de Centre des Recherches Exploration-Production ELF-Aquitaine*, **19**, 119–147.
Petit, S., Caillaud, J., Righi, D., Madejová, J., Elsass, F., and Köster, H.M. (2002) Characterization and crystal chemistry of an Fe-rich montmorillonite from Ölberg, Germany. *Clay Minerals*, **37**, 283–297.
Prost, R. and Chaussidon, J. (1969) The infrared spectrum of water adsorbed in hectorite. *Clay Minerals*, **8**, 143–149.
Ras, R.H.A., Umemura, Y., Johnston, C.T., Yamagishi, A., and Schoonheydt, R.A. (2007) Ultrathin hybrid films of clay minerals. *Physical Chemistry Chemical Physics*, **9**, 918–932.
Russell, J.D. and Farmer, V.C. (1964) Infrared spectroscopic study of the dehydration of montmorillonite and saponite. *Clay Minerals Bulletin*, **5**, 443–464.
Russell, J.D. and Fraser, A.R. (1994) Infrared methods. Pp. 11–67 in: *Clay Mineralogy: Spectroscopic and Chemical Determinative Methods* (M.J. Wilson, editor). Chapman and Hall, London.
Russell, J.D., Farmer, V.C., and Velde, B. (1970) Replacement of OH by OD in layer silicates, and identification of the vibrations of these groups in infra-red spectra. *Mineralogical Magazine*, **37**, 869–879.
Sándorfy, C. (2006) Hydrogen bonding: How much anharmonicity? *Journal of Molecular Structure*, **790**, 50–54.
Scatena, L.F., Brown, M.G., and Richmond, G.L. (2001) Water at hydrophobic surfaces: Weak hydrogen bonding and strong orientation effects. *Science*, **292**, 908–912.
Shen, Y.R. and Ostroverkhov, V. (2006) Sum-frequency vibrational spectroscopy on water interfaces: Polar orientation of water molecules at interfaces. *Chemical Reviews*, **106**, 1140–1154.
Sovago, M., Kramer Campen, R.K., Bakker H.J., and Bonn, M. (2009) Hydrogen bonding strength of interfacial water determined with surface sum-frequency generation. *Chemical Physics Letters*, **470**, 7–12.
Sposito, G. and Prost, R. (1982) Structure of water adsorbed on

smectites. *Chemical Reviews*, **82**, 554–573.
Sposito, G., Prost, R., and Gaultier, J.-P. (1983) Infrared spectroscopic study of adsorbed water on reduced-charge Na/Li-montmorillonites. *Clays and Clay Minerals*, **31**, 9–16.
Sposito, G., Skipper, N.T., Sutton, R., Park, S-H., Soper, A.K., and Greathouse, J.A. (1999) Surface geochemistry of clay minerals. *Proceedings of National Academy of Science USA*, **96**, 3358–3364.
Suquet, H., Prost, R., and Pezerat, H. (1977) Etude par la spectroscopie infrarouge de l' eau adsorbée par la saponite-calcium. *Clay Minerals*, **12**, 113–125.
Suzuki, S. and Kawamura, K. (2004) Study of vibrational spectra of interlayer water in sodium beidellite by molecular dynamics simulations. *Journal of Physical Chemistry B*, **108**, 13468–13474.
Tian C.S. and Shen Y.R. (2009) Sum-frequency vibrational spectroscopic studies of water/vapor interfaces. *Chemical Physics Letters*, **470**, 1–6.
Wang J., Kalinichev A.G., Kirkpatrick R.J., and Cygan R.T. (2005) Structure, energetics, and dynamics of water adsorbed on the muscovite (001) surface: A molecular dynamics simulation. *Journal of Physical Chemistry B*, **109**, 15893–15905.
Wolters, F., Lagaly, G., Kahr, G., Nueesch, R., and Emmerich, K. (2009) A comprehensive characterization of dioctahedral smectites. *Clays and Clay Minerals*, **57**, 115–133.
Xu, W., Johnston, C.T., Parker, P., and Agnew, S.F. (2000) Infrared study of water sorption on Na-, Li-, Ca- and Mg-exchanged (SWy-1 and SAz-1) montmorillonite. *Clays and Clay Minerals*, **48**, 120–131.
Yan, L.B., Roth, C.B., and Low, P.F. (1996) Changes in the Si-O vibrations of smectite layers accompanying the sorption of interlayer water. *Clays and Clay Minerals*, **12**, 4421–4429.
Zhang, L., Singh, S., Tian, C., Shen, Y.R., Wu, Y., Shannon, M., and Brinker, C.J. (2009) Nanoporous silica–water interfaces studied by sum-frequency vibrational spectroscopy, *The Journal of Chemical Physics*, **130**, 154702.
Zviagina, B.B., McCarty, D., Środoń, J., and Drits, V.A. (2004) Interpretation of infrared spectra of dioctahedral smectites in the region of OH-stretching vibrations. *Clays and Clay Minerals*, **52**, 399–410.

(*Received 31 July 2014; revised 11 February 2015; Ms. 905; AE: A.G. Kalinichev*)